Retinal pigment epithelial cells use a MerTK-dependent mechanism to limit the phagocytic particle binding activity of αvβ5 integrin

Emeline F. Nandrot[*,1], **Kathryn E. Silva**[†], **Christina Scelfo**[†], and **Silvia C. Finnemann**[*,†,2]

[*]Department of Ophthalmology, Margaret M. Dyson Vision Research Institute, Weill Medical College of Cornell University, New York, NY 10065, U.S.A.

[†]Department of Biological Sciences, Larkin Hall, Fordham University, Bronx, NY 10458, U.S.A.

Abstract

Background information—αvβ5 integrin and Mer tyrosine kinase (MerTK) receptors reside at the apical surface of the retinal pigment epithelium (RPE) in the eye to promote the diurnal, synchronised phagocytosis of shed photoreceptor outer segment fragments (POS) that is critical for vision. Phagocytosis assays studying RPE cells in culture have defined roles for αvβ5 in POS surface binding and for MerTK in engulfment of bound POS. Both receptors have thus far only been studied separately. It is therefore unknown if αvβ5 integrin activity in POS binding is independent of the engulfment function of RPE cells. This study investigates how increasing αvβ5 receptor levels affect POS binding and internalisation by wild-type (wt), αvβ5- or MerTK-deficient RPE.

Results—β5 integrin–green fluorescent protein (β5–GFP) fusion proteins formed heterodimeric receptors with endogenous αv integrin subunits at the apical surface of mouse or rat RPE cells that co-immunoprecipitated focal adhesion kinase and redistributed with bound POS such as endogenous αvβ5 receptors. In β5$^{-/-}$ RPE cells, de novo formation of αvβ5–GFP receptors restored POS binding and internalisation up to, but not, above wt POS uptake levels. In wt RPE cells, increasing levels of αvβ5 surface receptors by over-expressing β5–GFP only moderately stimulated POS binding, even if POS internalisation was inhibited pharmacologically or by lowering incubation temperatures. In contrast, the same increase in αvβ5 receptor levels dramatically enhanced POS binding of RPE cells lacking MerTK. Furthermore, decreasing MerTK expression by RNA interference increased POS binding to endogenous αvβ5 receptors of wt RPE cells.

Conclusions—Expressing β5–GFP is sufficient to reverse phagocytic deficiencies of RPE cells derived from β5$^{-/-}$ mice, indicating that these cells do not irreversibly lose other components of the phagocytic machinery. RPE cells expressing the engulfment receptor MerTK control POS binding by limiting activity of endogenous αvβ5 and αvβ5–GFP integrins, although they reside at the apical, phagocytic surface. In contrast, RPE cells permanently or transiently losing MerTK expression lack this regulatory mechanism and bind excess POS via surface αvβ5 receptors.

[2]To whom correspondence should be addressed (finnemann@fordham.edu).
[1]Current address: Institut de la Vision, INSERM U968, UPMC Univ Paris 06, UMR_S 968, CNRS UMR_7210, 17 rue Moreau, Paris F-75012, France.

Conflict of interest statement
The authors have declared no conflict of interest.

Taken together, these data reveal a novel feedback mechanism that restricts binding of POS to surface αvβ5 integrin receptors in RPE cells.

Keywords

αvβ5 Integrin; Binding; Phagocytosis; Receptor activity; Retinal pigment epithelium

Introduction

Renewal of photoreceptor rod and cone outer segments in the retina involves continuous synthesis of new membranous disks and circadian shedding of most aged, distal tips (Young, 1967). Prompt and complete clearance phagocytosis of spent photoreceptor outer segment fragments (POS) by the underlying retinal pigment epithelium (RPE) is crucial for retinal function and photoreceptor survival (Young and Bok, 1969).

Our previous studies have identified the integrin receptor αvβ5 and its ligand MFG-E8 as a major molecular mechanism used by RPE cells to recognise phagocytic particles (Nandrot et al., 2004, 2007). β5$^{-/-}$ mice lacking αvβ5 integrin retain phenotypically normal RPE with basal levels of engulfment activity but completely lack the diurnal peak of uptake that is characteristic to wild-type (wt) RPE. Furthermore, phosphorylation levels of two tyrosine kinases with roles in engulfment, focal adhesion kinase (FAK) and Mer tyrosine kinase (MerTK), fluctuate in wt but not in β5$^{-/-}$ RPE *in vivo*.

Retinal pigment epithelium cells in culture retain vigorous phagocytic activity towards isolated POS that depends on αvβ5, FAK and MerTK. Binding and engulfment steps of phagocytosis can be separated experimentally by choosing appropriate time points for analysis or by differentiating surface bound from internal POS (Finnemann and Rodriguez-Boulan, 1999; Mayerson and Hall, 1986). *In vitro* phagocytosis assays have demonstrated that lack of αvβ5 in primary RPE derived from β5$^{-/-}$ mice severely reduces POS binding and engulfment (Nandrot et al., 2004). RPE cells derived from rats or mice lacking functional MerTK show normal αvβ5 integrin expression and POS binding but fail to engulf surface-tethered POS (Chaitin and Hall, 1983a; Feng et al., 2002; Finnemann, 2003).

These *in vivo* and *in vitro* findings suggest that MerTK activation by RPE cells depends on αvβ5 integrin/FAK. However, it is also possible that the constitutive lack of αvβ5 integrin has caused permanent secondary changes in signalling or phagocytic proteins in β5$^{-/-}$ RPE that may be responsible for their lack of MerTK stimulation and phagocytosis in response to POS. Furthermore, it has not yet directly been studied if POS binding by αvβ5 receptors is independent of the rest of the RPE phagocytic machinery or if levels of POS binding are controlled by RPE cells to match their engulfment capacity.

In this study, we generated a recombinant adenovirus expressing the complete human β5 integrin protein coupled to green fluorescent protein (GFP) to directly test the effect of re-expression of β5 integrin on β5$^{-/-}$ RPE phagocytic activity. Our results show that expressing β5 integrin–GFP (β5–GFP) in β5$^{-/-}$ RPE fully restores POS binding and POS engulfment. Furthermore, we used the β5–GFP adenovirus to test if increasing αvβ5 integrin levels is sufficient to enhance POS binding and engulfment by RPE cells. We found that increasing αvβ5 in the stable rat RPE-J cell line or wt primary, unpassaged RPE from rats or mice has little effect on POS binding or engulfment. In contrast, increasing αvβ5 integrin levels in Royal College of Surgeons (RCS) RPE that lacks functional MerTK (D'Cruz et al., 2000; Nandrot et al., 2000) dramatically increases POS binding. Reducing MerTK expression by RNA interference increased POS binding to endogenous αvβ5 integrin in RPE-J cells but inhibiting POS internalisation by reducing the assay temperature

or with tyrosine kinase inhibitors did not. Taken together, these results imply that the POS binding function of αvβ5 integrin is limited by a novel MerTK-dependent mechanism in wt RPE.

Results and discussion

Human β5–GFP integrin forms chimeric receptors with rat or mouse αv integrin subunits that increase total αvβ5 receptor levels at the apical surface of RPE cells

Integrins form a large family of heterodimeric receptors composed of one α and one β integrin subunits each. We took advantage of the fact that β5 subunits only dimerise with αv subunits to target specifically αvβ5 receptors in our study. We constructed an expression plasmid encoding a chimeric protein composed of the full-length human β5 integrin subunit fused with GFP at its carboxiterminus (β5–GFP).Singh et al. (2007) had shown earlier that transient transfection of an equivalent construct encoding β5–GFP yielded surface αvβ5–GFP receptors in human HeLa and hamster CS-1 cells. To test whether human β5–GFP proteins also form dimers with mouse and rat αv subunits, we transiently transfected mouse and rat cell lines with our β5–GFP construct or control plasmid encoding soluble GFP. Live labelling of chilled cells with a monoclonal αvβ5 antibody P1F6 showed surface labelling of mouse 3T3 fibroblasts expressing β5–GFP but not soluble GFP (Figure 1A). P1F6 antibody recognises intact rat or human αvβ5 heterodimers but not single β5 subunits or mouse αvβ5 heterodimers (Wayner et al., 1991). Although αvβ5 heterodimer-specific labelling co-localised with β5–GFP fluorescence at the cell surface, we observed additional β5–GFP in intracellular compartments, likely the endoplasmic reticulum and Golgi apparatus. Thus, human β5 integrin forms heterodimers with mouse αv integrin that traffic to the cell surface. Furthermore, the mouse αv/human β5 chimeric receptor is recognised by the monoclonal antibody P1F6. This suggests that P1F6 fails to bind to mouse αvβ5 because of epitope differences between human and mouse β5 subunits.

In polarised RPE cells in culture and in the RPE in the eye, αvβ5 integrins localise to the apical surface, whereas all other RPE integrins studied to date localise basolaterally (Anderson et al., 1995; Finnemann et al., 1997). Here, we tested P1F6 αvβ5 receptor labelling of the rat RPE-J cell line that was transiently transfected with GFP or β5–GFP following formation of a polarised monolayer. In these cells, P1F6 labelled endogenous surface αvβ5 receptors (Figure 1B). In cells that fluoresced green indicating β5–GFP expression, we observed stronger labelling with P1F6 antibody, suggesting that increasing protein levels of β5 integrin subunits by transfection is sufficient to increase overall αvβ5 surface receptor levels in these cells.

Taken together, these data show that human β5– GFP fusion proteins form cell surface heterodimeric receptors with both mouse and rat αv integrin proteins. Furthermore, αvβ5–GFP integrin receptors localise to the apical, phagocytic surface of polarised rat RPE cells, such as endogenous αvβ5.

Because of very low transfection rates of polarised RPE cells, we custom ordered a recombinant adenovirus expressing our β5–GFP construct and transduced cells using purified β5–GFP or soluble GFP adenovirus. First, we used our new adenovirus to determine the effect of β5–GFP expression on the quantity of αvβ5 receptors available at the apical surface of RPE-J cells. Like before, for αvβ5 surface fluorescence detection, we again labelled apical surface αvβ5 and αvβ5–GFP with P1F6 antibody in live, chilled cells. We then lysed the cells and quantified the amount of surface αv subunit recognised by P1F6 by immunoblotting (Figures 2A and 2B, panel surface). This surface immunoisolation procedure did not yield αv protein non-specifically as control samples incubated with non-immune IgG did not contain αv (Figure 2A). We also immunoisolated total cellular αvβ5/

αvβ5–GFP by standard immunoprecipitation from whole cell lysates (Figure 2B, panel total). Densitometry revealed that β5–GFP expression increased levels of αvβ5 receptors at the cell surface and of total cellular αvβ5 receptors to the same extent (Figure 2C). POS incubation for 1.5 or for 3.5 h had no effect on total or cell surface levels of αvβ5 receptors, regardless whether cells expressed αvβ5 only or αvβ5 and αvβ5–GFP. These data demonstrate that RPE cells are able to efficiently and significantly increase levels of αvβ5 receptors available at the cell surface by incorporating exogenous β5–GFP.

αvβ5–GFP receptors form a complex with FAK and re-localise with POS challenge in RPE cells such as endogenous αvβ5

Because of their superior expression efficiency and lower levels of toxicity, we used the recombinant adenovirus to express β5–GFP for all further experiments studying RPE cells.

Next, we investigated whether αvβ5–GFP integrin receptors interact with other cellular proteins such as endogenous αvβ5 in RPE cells. We showed previously that αvβ5 integrin receptors reside in a complex with FAK in RPE cells (Finnemann, 2003). To characterise proteins specifically associated with β5–GFP, we used GFP antibodies to immunoprecipitate β5–GFP complexes from RPE-J cells infected with β5–GFP adenovirus (Figure 3A). Control cells received GFP adenovirus. GFP immunoprecipitation was successful as we detected immunoisolated β5– GFP with antibodies to GFP or to β5 in β5–GFP transduced cells. As expected, we detected GFP protein with GFP antibodies only in GFP-transduced cells. Furthermore, β5–GFP but not GFP immunoprecipitations contained αv integrin and FAK. All proteins detected were specifically isolated by the GFP antibody as none was present in control immunoprecipitations with non-immune antibody.

αvβ5 integrin receptors at the surface of RPE-J cells re-localise to sites of POS particles during experimental phagocytosis assays (Finnemann et al., 1997). Here, we challenged β5– GFP-expressing RPE-J cells with isolated POS for 1 h. Figure 3B shows that surface αvβ5 receptors labelled in live chilled cells with P1F6 αvβ5 receptor antibody (red) co-localised with the POS particle (blue) associated with the cell. Partial overlap of GFP with αvβ5 receptor and POS labels suggested that αvβ5–GFP contributes to the αvβ5 receptor recruited to the particle. The reconstructed x–z plane section of the same field further confirmed joint enrichment of β5–GFP and αvβ5 labels at the site of surface-bound POS.

Taken together, αvβ5–GFP receptors associate with FAK and re-localise in response to POS incubation in RPE cells such as endogenous αvβ5. Thus, fusion of globular GFP with the β5 integrin cytoplasmic domain and chimeric receptor formation of rodent αv with human β5–GFP does not abolish receptor properties known to be important for POS phagocytosis.

Over-expression of αvβ5 receptors does not proportionally increase POS phagocytosis

Next, we set out to investigate the effect of extra αvβ5 receptors on expression of other proteins of the phagocytic machinery of RPE cells (Figure 4A). We over-expressed β5–GFP or GFP control using two different concentrations of each virus that we will refer to as low or high dose. The high dose was the same effective dose used above (Figures 2 and 3). The low dose contained half the number of virus particles compared with the high dose. Both doses significantly increased total cellular β5 integrin protein levels. The low dose yielded half as much β5–GFP protein as the high dose. Thus, virus dose correlated directly with levels of exogenous protein expression. Expression levels of endogenous β5 subunits were not significantly affected by either virus, regardless of dose. αv subunit steady-state protein levels increased in response to both low and high β5–GFP expression as compared with GFP. This suggests increased αv integrin production or slower turnover of αv subunits when engaged in αvβ5 integrin dimers. MerTK levels were also increased in low and high

β5–GFP expressing samples by about one third on average, but this increase varied amongst experiments and did not reach statistical significance. Levels of actin as well as of ezrin, an RPE-specific protein localised at the apical surface, remained similar in all samples. Thus, virus transduction and over-expression did not cause a gross change in cell structure. Dependence of αv steady-state levels on β5/β5–GFP levels detected here fits well to our earlier findings that β5$^{-/-}$ eyecups possess only half as much αv integrin as wt RPE, whereas no other integrin subunit is affected (Nandrot et al., 2006). These observations suggest that αv and β5 protein levels are linked in RPE cells independently of other β integrin subunits.

We next quantified POS binding and internalisation by fluorescence scanning. We chose to quantify POS uptake after 1.5 h, a time at which mainly POS binding takes place, and after 3.5 h, a time at which both POS binding and POS internalisation are active in RPE-J cells (Finnemann et al., 1997). Cells expressing low levels of β5–GFP did not differ in total (bound plus internal POS content) after 1.5 h but took up 51% more POS than cells expressing GFP by 3.5 h (Figure 4B). Likewise, high dose of β5–GFP moderately (by 46% on average) but significantly increased total POS uptake by 3.5 h (Figure 4C) compared with high dose GFP. Cells expressing high dose β5–GFP did not significantly differ in total POS uptake at either time point from cells expressing low dose β5–GFP. Figure 4D shows that all cells engulfed similar fractions of total POS by 3.5 h regardless of over-expression. Taken together, increasing surface levels of αvβ5 by expressing β5–GFP had only a moderate effect on total POS phagocytosis. Lack of change in internalisation ratio suggests that POS binding and POS engulfment were enhanced to similar extent. Thus, increased levels of surface POS in β5–GFP expressors do not persist at the cell surface but are efficiently engulfed. Total POS uptake did not increase to the same extent as β5 integrin expression levels. These data suggest that the phagocytic capacity of RPE-J cells is limited by factors other than the availability of β5 integrin.

Expression of β5–GFP is sufficient to restore apical αvβ5 receptor expression and POS phagocytosis by β5$^{-/-}$ RPE cells

The RPE-J cell line possesses and employs the phagocytic machinery via αvβ5, FAK and MerTK, but their rate and capacity of POS phagocytosis are reduced compared with primary RPE cells. We, therefore, tested if increasing β5 integrin levels may be more effective in enhancing POS uptake by primary RPE. We examined side-by-side unpassaged primary RPE isolated in multi-cell patches from wt or β5$^{-/-}$ mice. Primary mouse RPE derived from wt mice showed efficient expression of β5–GFP or GFP upon adenoviral infection and formation of apical surface αvβ5–GFP receptors (data not shown). Figure 5 shows that synthesis of β5–GFP, but not of GFP alone, also promotes *de novo* expression of αvβ5–GFP heterodimers at the apical surface of primary β5$^{-/-}$ RPE. Thus, β5$^{-/-}$ RPE cells do not harbour deficiencies that preclude restoration of αvβ5 receptor formation with correct receptor polarity. We next transduced wt and β5$^{-/-}$ primary RPE cells with low and high dose adenovirus expressing GFP alone or β5–GFP. Immunoblotting confirmed that low and high dose gave rise to low and high levels of β5–GFP in both types of primary RPE (Figures 6A and 6B). We noted some β5 protein of the molecular size of untagged β5 and soluble GFP upon over-expressing β5–GFP, suggesting that a minor fraction of β5– GFP protein loses its GFP tag. Extra β5–GFP did not affect protein expression in general as MerTK and actin levels remained unchanged. Levels of the αv integrin subunit changed little in wt RPE but increased to wt levels in β5$^{-/-}$ RPE upon expression of β5–GFP (Figure 6A) in agreement with our observations in RPE-J cells (Figure 4). Mean levels of exogenous protein expression were similar in wt and β5$^{-/-}$ RPE with high dose virus infection, resulting in about 10-fold higher β5–GFP or GFP steady-state protein levels than low dose virus (Figure 6B). To test effects of β5–GFP on POS uptake, we fed cells with POS for 1 h

followed by cell lysis and immunoblotting for opsin, a protein exclusively expressed in POS (Figures 6C and 6D show representative immunoblots). Wt cells transduced with low dose β5–GFP virus did not differ in POS uptake from cells expressing low dose GFP (Figures 6C, 6E and 6F). This was true, quantifying total (bound plus internal) POS or internalised POS alone. Even high dose β5–GFP expression increased total and internalised POS on average by only 25% and 35%, respectively. Thus, over-expressing β5–GFP in highly phagocytic wt mouse primary RPE had little effect on POS uptake. In contrast, β5–GFP expression dramatically improved the phagocytic capacity of β5$^{-/-}$ RPE at both low and high doses (Figures 6D–6F). Low levels of β5–GFP increased total and internal POS of β5$^{-/-}$ RPE to 71% and 55% of POS of wt RPE expressing low levels of β5–GFP. High levels of β5–GFP completely restored levels of total and internal POS taken up by β5$^{-/-}$ RPE but, notably, did not cause excess uptake. These data show that expression of β5–GFP causes β5$^{-/-}$ RPE to regain POS binding and engulfment function equal to that of wt RPE. It is important to note, however, that expression of β5–GFP and/or formation αvβ5 receptors may induce additional changes in β5$^{-/-}$ RPE that may also contribute to their phagocytic activity. Comparison of transcriptional or protein expression profiles of β5$^{-/-}$ RPE before and after β5–GFP induction would be informative but are beyond the scope of the current study. Both wt and β5$^{-/-}$ RPE levels of total and internal POS increase little with higher levels of β5–GFP. The POS uptake capacity of primary mouse RPE cells, such as uptake of RPE-J cells, is thus likely limited by molecules other than the β5 integrin subunit.

Expression of β5–GFP causes excess POS binding by MerTK-deficient (RCS) but not by wt rat primary RPE

Next, we tested if β5–GFP functionality was related to the engulfment machinery involving MerTK. We repeated the β5–GFP over-expression analysis comparing wt rat RPE cells with MerTK-deficient RPE cells derived from the RCS rat. Low and high doses of GFP and β5–GFP virus yielded considerable protein over-expression with negligible effect on endogenous β5 and αv integrins, MerTK or actin (Figures 7A and 7B). As observed earlier for wt mouse RPE, even high dose of β5–GFP had little impact on POS uptake by wt rat RPE, increasing total or internal POS by 22% compared with low dose β5–GFP expression (Figures 7C, 7E and 7F). We did not detect opsin fragmentation in wt RPE samples after 1.5 h of POS challenge, indicating that loss of POS marker by digestion was insignificant (data not shown). The effects of β5–GFP expression on POS uptake by MerTK-deficient RPE were completely different: low dose β5–GFP increased total POS fivefold compared with low dose GFP. Compared with low dose β5–GFP, high dose β5–GFP increased total POS taken up by RCS RPE by 415% (Figures 7D, 7E and 7F). RCS RPE took up 4.1-fold more total POS than wt RPE if both expressed similar, high levels of β5–GFP (Figures 7E and 7F). This dramatic increase in total POS reflected increases in POS binding alone as RCS RPE cells continued to fail to internalise bound POS, regardless of protein over-expression (Figures 7D and 7F). Thus, expressing αvβ5–GFP receptors does not activate particle engulfment independent of MerTK. However, increasing β5–GFP levels in MerTK-deficient RPE cells cause a significantly larger increase in POS binding than increasing β5–GFP levels in wt RPE.

Levels of surface αvβ5/β5–GFP receptors of RCS and wt primary RPE expressing β5–GFP are similar and remain unchanged upon POS challenge

We wondered whether RCS RPE bound more POS because they formed or retained during POS challenge more surface αvβ5–GFP receptors than wt RPE. We therefore quantified αvβ5/β5–GFP receptor levels at the apical, phagocytic surface by incubating live, chilled wt and RCS RPE expressing high level of β5–GFP after challenge with medium or POS with αvβ5 heterodimer antibody, followed by precipitation of immune complexes. Both cell types contained similar total levels of β5/β5–GFP and αv integrin subunits in Figure 8A.

Neither integrin (nor MerTK in wt RPE) changed in response to POS challenge (Figure 8A, compare lanes m with lanes POS). We detected equal levels of αv integrin in immunoprecipitates of both cell types (Figure 8B). Cells fed with POS carried approximately 10% less surface αv than cells fed with medium, but this difference was small, did not reach statistical significance and was observed in both wt and RCS RPE. These data indicate that wt and RCS RPE possess the same total level of αvβ5/αvβ5–GFP receptors at their apical plasma membranes. Thus, excess POS binding by RCS RPE is not a result of increased abundance of surface αvβ5 receptors at the phagocytic surface.

Inhibiting internalisation of surface-bound POS fails to upregulate POS binding by wt RPE expressing β5–GFP

MerTK deficiency directly causes a failure of RCS RPE in internalisation of bound POS. We thus suspected that increased binding of POS by RCS RPE may be a secondary effect of the internalisation defect. To test this possibility, we separately analysed binding and engulfment phases of POS uptake by wt and RCS RPE expressing β5–GFP. Pulse–chase experiments take advantage of different temperature requirements of binding and internalisation processes. Addition of POS to RPE at 20°C allows POS surface binding via αvβ5 receptors but not engulfment (pulse; #687) (Finnemann, 1999). Following removal of unbound POS, further incubation at 37°C allows RPE cells to internalise POS pre-bound during the pulse (chase). Figure 9 illustrates the outcome of such pulse–chase experiments comparingwt and RCSRPE both expressing high levels of β5–GFP. During the pulse, RCS RPE bound significantly more POS than wt RPE, although both wt and RCS RPE did not internalise POS (Figure 9, compare lane 1 with 5). During the chase, wt but not RCS RPE internalised pre-bound POS, as expected (Figure 9, compare lane 4 with 3 and 8 with 7). Notably, there was negligible net loss of total POS–opsin during the chase period in both cell types, indicating that wt RPE did not digest phagocytosed POS–opsin and that RCS RPE did not release surface-bound POS during the chase period (Figure 9, compare lane 4 with 1 and 7 with 5). Taken together, the pulse–chase assays revealed that excess POS binding by RCS RPE cells is not a mere consequence of their failure to internalise POS.

Reducing MerTK expression but not inhibiting internalisation in RPE-J cells with normal levels of MerTK increases POS binding by endogenous αvβ5 receptors

Finally, we set out to extend these intriguing observations by testing whether MerTK expression and engulfment activity affect POS binding via endogenous αvβ5 receptors. To this end, we challenged RPE-J cells with POS while either inhibiting POS internalisation acutely (by incubating at 20°C or pharmacologically with Herbimycin A) or following transient reduction of MerTK expression (with siRNA). Neither lower temperature nor the tyrosine kinase inhibitor Herbimycin A altered expression levels of αv integrin, β5 integrin or MerTK (Figure 10A). A 2-day treatment of RPE-J cells with MerTK-specific siRNA decreased MerTK protein levels significantly by $76 \pm 12\%$ on average ($n = 3$) but left integrin expression unaffected (Figure 10A). MerTK downregulation was the sole condition tested that significantly altered POS binding during 3.5 h of phagocytic challenge, increasing the numbers of bound POS 4.8-fold compared with cells treated with control siRNA (Figure 10B). Blocking αvβ5 integrin with antibody during POS challenge considerably reduced POS binding of all cells including cells with less MerTK (Figure 10C). 20°C temperature, Herbimycin A and MerTK downregulation decreased the fraction of POS internalised during the assay period, confirming that all three experimental manipulations inhibited POS internalisation as intended (Figure 10D). Taken together, these results show that lowering expressing of MerTK augments POS binding by RPE in an αvβ5 integrin-dependent manner. They confirm that RPE cells increase POS binding due to lack of MerTK specifically rather than as a response to lack of engulfment. We therefore propose that MerTK acts a novel negative regulator of αvβ5 integrin, limiting POS binding by RPE cells.

Conclusions

Our results shed new light on the relationship between αvβ5 integrin and MerTK during POS phagocytosis by RPE cells. They demonstrate that restoring β5 integrin expression is sufficient to fully rescue the POS binding and engulfment defect of β5$^{-/-}$ RPE. Furthermore, POS tethering to αvβ5 receptors at the phagocytic surface is limited in RPE cells with intact MerTK-dependent engulfment machinery, suggesting an RPE-intrinsic control mechanism. POS binding and POS engulfment are separable steps of RPE phagocytosis, each one of which can be saturated in cell culture assays (Mayerson and Hall, 1986). Our data suggest that RPE cells limit the number of POS particles they tether by regulating αvβ5 receptor binding activity, independently of receptor surface expression levels. It is possible that regulation of POS binding occurs at the level of integrin receptor activation itself, for example by inside-out signalling affecting integrin anchorage or interaction with cytoplasmic-associated proteins (Finnemann and Rodriguez-Boulan, 1999). In RCS RPE, lack of MerTK itself or of other aspects of MerTK-dependent POS engulfment results in excess POS surface binding. Transient reduction in RPE-J cells of MerTK expression similarly increases αvβ5-dependent POS binding. These data imply that RPE cells lacking MerTK fail to restrict POS binding. Such inactivation is not a mere consequence of reduced engulfment because inhibition of engulfment pharmacologically or by lowering incubation temperatures does not mimic the effect of loss of MerTK. Mechanistically, our data indicate that steady-state αvβ5 surface receptor levels are independent of MerTK. MerTK may affect αvβ5 anchorage either to other plasma membrane components such as CD81 (Chang and Finnemann, 2007) or to the sub-apical cytoskeleton. RCS RPE cells do not exhibit obvious defects in actin or tubulin cytoskeletal systems (Chaitin and Hall, 1983b; Irons and Kalnins, 1984). We speculate that MerTK signalling may alter αvβ5 integrin-associated proteins with roles in αvβ5 anchorage. MerTK's signalling functions are only poorly understood. MerTK signalling can activate FAK, promoting αvβ5 function in apoptotic cell phagocytosis in transfected fibroblasts (Wu et al., 2005). Conversely, αvβ5/FAK signalling is required for efficient MerTK activation during POS phagocytosis by RPE *in vitro* and *in vivo* (Finnemann, 2003; Nandrot et al., 2004). Clearly, the crosstalk of αvβ5 and MerTK in RPE cells is complex. Future studies are needed to unravel the precise signalling pathways and intermediates that connect these two surface receptors in phagocytic mechanisms.

Materials and methods

Expression plasmid and adenovirus generation

The complete human β5 integrin cDNA (kindly provided by D.A. Cheresh, Scripps Research Institute) was amplified by polymerase chain reaction (PCR) using forward 5′-CTCGAGCATGCCGCGGGCCCCGGCGCCGCTGTACGC and reverse 5′-GGATCCAGTCCACAGTGCCATTGTAGGATTTGTTG primers removing the stop codon and generating restriction sites for further sub-cloning. PCR products ligated into pCR2.1 TOPO vector (Invitrogen) were sequenced (Bioresource Center, Cornell University) and one verified clone was digested with XhoI and BamHI (New England Biolabs, gel-purified using the GeneClean III kit (Bio 101 Systems, Qbiogene) and inserted into the pEGFP-N2 vector (Clontech) to generate a construct encoding a β5–GFP fusion protein.

We obtained crude lysates from two custom-made β5–GFP pLEPCMV adenovirus clones (Welgen Inc.). Control GFP adenovirus was a kind gift from Dr E. Rodriguez-Boulan (Weill Cornell Medical College). Confluent HEK 293 cells (70%; ATCC) were transduced with GFP or β5–GFP adenovirus and harvested after 3 days. We followed a published protocol to purify GFP and β5–GFP virus stocks using CsCl gradients (Falck-Pedersen, 1998). Purified viruses were dialysed against 0.1 M Tris pH 7.5, 0.25M NaCl, 10% glycerol buffer and stored long-term diluted to 50% glycerol concentration at −20°C.

Cell culture, siRNA knockdown and adenovirus infection

3T3 fibroblasts (ATCC) and HEK 293 cells were grown at 37°C, 5% CO_2 in Dulbecco's modified Eagle's medium (DMEM) or improved modified Eagle's medium, respectively, supplemented with 10% foetal bovine serum (FBS), L-glutamine and sodium pyruvate. Rat RPE-J cells (ATCC) were maintained at 32°C, 5% CO_2 in DMEM supplemented with 4% FBS (CELLect Gold, ICN). Cell lines were transduced for 3.5 h with either GFP or β5–GFP adenovirus at $1.5–7 \times 10^9$ particles per millilitre. Cell lines were transfected with plasmid DNA using FuGENE 6 reagent (Roche) or with siRNA using Lipofectamine 2000 (Invitrogen) according to the manufacturer's protocols. To silence MerTK expression, RPE-J cells received a mixture of four different 21-nucleotide RNAs specifically targeting rat MerTK (Mission R ® siRNA; Sigma). Control non-targeting siRNA with at least four mismatches to any human, mouse or rat gene were also from Sigma. RPE cells from 10-to-12-day-old wt and β5−/5 mice or wt Long Evans and RCS rats for primary culture were isolated as previously published in detail (Finnemann, 2003; Nandrot et al., 2004). Purified RPE patches were grown on serum-coated glass coverslips or in 96-well plates in DMEM, 10% FBS at 37°C, 10% CO_2 for 5–7 days before experiments. Primary RPE cells were infected with $1.5–3.5 \times 10^9$ adenovirus particles per millilitre for 4 h and used for experiments 1–2 days later. All procedures involving animals adhered to the ARVO Statement for the Use of Animals in Ophthalmic and Vision Research and were approved by the Weill Medical College and the Fordham University Institutional Animal Care and Use Committees.

Immunofluorescence staining and microscopy

Cells on glass coverslips were fixed in 4% paraformaldehyde in phosphate-buffered saline (PBS) with 0.2 mM $CaCl_2$, 1 mM $MgCl_2$ (PBS–CM) for 20 min at room temperature. Excess fixative was quenched with 50 mM NH_4Cl PBS–CM. Non-specific signals were blocked in 1% bovine serum albumin in PBS– CM before sequential incubation with primary and secondary antibodies (AlexaFluor series; Invitrogen) for at least 1 h each, labelling of nuclei with 4′,6-diamidino-2-phenylindole, dihydrochloride (DAPI) and mounting with Fluoromount G (SouthernBiotech). POS were labelled with rabbit anti-rat POS antibodies (a gift from M.O. Hall, UCLA). Surface αvβ5 integrin receptors were assessed by live labelling of pre-chilled cells for 45 min on ice with αvβ5 heterodimer-specific monoclonal antibody P1F6 (Covance) at 20 μg/ml before subsequent fixation and processing as detailed above. x–y stacks were acquired at 0.2 μm intervals using either 40× or 63× objectives at room temperature on a Leica TSP2 confocal microscopy system and recompiled in Photoshop 7.0.

Cell lysis, immunoprecipitations and immunoblotting

Cells were lysed with 50 mM N-2-hydroxyethylpiperazine-N′- 2-ethane sulfonic acid (pH 7.4), 150 mM NaCl, 10% glycerol, 1.5 mM $MgCl_2$, 1% Triton X-100, freshly supplemented with 1% of protease and phosphatase inhibitor cocktails (Sigma).

To collect surface αvβ5 immune complexes, cells in 24-well plates were rinsed three times with ice-cold PBS–CM, incubated with 20 μg/ml P1F6 or control non-immune mouse IgG diluted in Hank's saline for 45 min on ice, washed three times with ice-cold PBS–CM and lysed. To collect total αvβ5 or GFP immune complexes, pre-cleared cell lysates were incubated with 1 μg of P1F6, goat anti-GFP (Rockland Immunochemicals) or nonimmune mouse or goat IgG for 3 h at 4°C. Immune complexes were collected by adding Protein L agarose (Sigma) or ImmunoPure Immobilised Protein G (Pierce) beads for 2 h at 4°C. Beads were washed three times in lysis buffer without detergent before elution of proteins in reducing sample buffer.

We separated whole cell lysates representing 10,000 RPE cells or immunoprecipitates on 10% sodium-dodecyl sulfate– polyacrylamide (SDS) gels. Nitrocellulose blotting membranes were probed for actin, ezrin (both Sigma), αv integrin (BD Biosciences), β5 integrin, FAK (both Santa Cruz Biotechnologies), GFP (Rockland), MerTK (R&D Systems), RPE65 (Millipore) and opsin (a kind gift from Paul Hargrave, University of Florida) (Adamus et al., 1991), and incubated with appropriate horseradish peroxidase-conjugated secondary antibodies followed by ECL chemiluminescence detection (PerkinElmer). X-ray films were scanned and processed using Photoshop 7.0 (Adobe). Signals were quantified using ImageJ 1.36b software (NIH).

POS phagocytosis assays

POS were purified from bovine or porcine eyes obtained fresh from the slaughterhouse and labelled with fluorescein isothiocyanate (FITC) dye (Invitrogen) as described earlier (Finnemann et al., 1997). RPE cells were challenged with approximately 10 POS per cell in DMEM with 5% FBS for the duration of the experiment, chilled, washed three times with PBS–CM to remove excess POS, and lysed or fixed in ice-cold methanol. For pulse–chase experiments, cells were incubated with POS at 20°C for 1 h. Following removal of unbound POS and two washes in serum-free DMEM, cells received fresh DMEM with 5% FBS and were further incubated for 1 h before analysis. Tyrosine kinase inhibitor Herbimycin A at 20 μM (EMD Biosciences) or αvβ5 antibody P1F6 at 25 μg/ml were included for the duration of POS challenge in selected assays. FITC–POS fluorescence of coverslips mounted on glass slides was recorded using a Typhoon Trio scanner and quantified using ImageQuant 1.2 (Finnemann et al., 1997). Bound POS were calculated by subtracting internal from total POS.

To assess RPE phagocytic function by immunoblotting, we quantified opsin as marker protein for POS and calculated opsin–actin ratios. To quantify total (bound plus internal) POS, samples were washed three times with PBS–CM before lysis. To quantify internal POS only, samples were incubated with 2 mM ethylenediaminetetraacetic acid (EDTA) in PBS for 10 min at room temperature, followed by three washes in PBS to remove POS bound at the cell surface prior to cell lysis.

Statistical analysis

All experiments were performed at least three times independently. In each phagocytosis assay, triplicate samples were analysed. Student's t-test was used for statistical analysis. $P <$ 0.05 was considered to indicate significant difference.

Acknowledgments

Abbreviations used

β5$^{-/-}$ β5 integrin knockout

FAK focal adhesion kinase

| GFP	green fluorescent protein
MerTK	Mer tyrosine kinase
PBS–CM	phosphate-buffered saline with 0.1 mM $CaCl_2$ and 1 mM $MgCl_2$
POS	shed photoreceptor outer segment fragments
RCS	Royal College of Surgeons
RPE	retinal pigment epithelium
wt	wild-type.

References

Adamus G, Zam ZS, Arendt A, Palczewski K, McDowell JH, Hargrave PA. Anti-rhodopsin monoclonal antibodies of defined specificity: Characterization and application. Vision Res. 1991; 31:17–31. [PubMed: 2006550]

Anderson DH, Johnson LV, Hageman GS. Vitronectin receptor expression and distribution at the photoreceptor–retinal pigment epithelial interface. J Comp Neurol. 1995; 360:1–16. [PubMed: 7499556]

Chaitin MH, Hall MO. Defective ingestion of rod outer segments by cultured dystrophic rat pigment epithelial cells. Invest Ophthalmol Vis Sci. 1983a; 24:812–820. [PubMed: 6345445]

Chaitin MH, Hall MO. The distribution of actin in cultured normal and dystrophic rat pigment epithelial cells during the phagocytosis of rod outer segments. Invest Ophthalmol Vis Sci. 1983b; 24:821–831. [PubMed: 6345446]

Chang Y, Finnemann SC. Tetraspanin CD81 is required for the $\alpha v \beta 5$ integrin-dependent particle-binding step of RPE phagocytosis. J Cell Sci. 2007; 120:3053–3063. [PubMed: 17684062]

D'Cruz PM, Yasumura D, Weir J, Matthes MT, Abderrahim H, LaVail MM, Vollrath D. Mutation of the receptor tyrosine kinase gene Mertk in the retinal dystrophic RCS rat. Hum Mol Genet. 2000; 9:645–651. [PubMed: 10699188]

Falck-Pedersen, E. Use and application of adenovirus expression vectors. In: Spector, DL.; Goldman, R.; Leinwand, L., editors. Cells: A laboratory manual, Vol. II, section 8. Cold Spring Harbor, NY, USA: Cold Spring Harbor Laboratory Press; 1998.

Feng W, Yasumura D, Matthes MT, LaVail MM, Vollrath D. Mertk triggers uptake of photoreceptor outer segments during phagocytosis by cultured retinal pigment epithelial cells. J Biol Chem. 2002; 277:17016–17022. [PubMed: 11861639]

Finnemann SC. Focal adhesion kinase signaling promotes phagocytosis of integrin-bound photoreceptors. EMBO J. 2003; 22:4143–4154. [PubMed: 12912913]

Finnemann SC, Bonilha VL, Marmorstein AD, Rodriguez-Boulan E. Phagocytosis of rod outer segments by retinal pigment epithelial cells requires $\alpha v \beta 5$ integrin for binding but not for internalization. Proc Natl Acad Sci U S A. 1997; 94:12932–12937. [PubMed: 9371778]

Finnemann SC, Rodriguez-Boulan E. Macrophage and retinal pigment epithelium phagocytosis: Apoptotic cells and photoreceptors compete for $\alpha v \beta 3$ and $\alpha v \beta 5$ integrins, and protein kinase C regulates $\alpha v \beta 5$ binding and cytoskeletal linkage. J Exp Med. 1999; 190:861–874. [PubMed: 10499924]

Irons MJ, Kalnins VI. Distribution of microtubules in cultured RPE cells from normal and dystrophic RCS rats. Invest Ophthalmol Vis Sci. 1984; 25:434–439. [PubMed: 6368459]

Mayerson PL, Hall MO. Rat retinal pigment epithelial cells show specificity of phagocytosis *in vitro*. J Cell Biol. 1986; 103:299–308. [PubMed: 3522605]

Nandrot E, Dufour EM, Provost AC, Pequignot MO, Bonnel S, Gogat K, Marchant D, Rouillac C, Sepulchre de Conde B, Bihoreau MT, Shaver C, Dufier JL, Marsac C, Lathrop M, Menasche M, Abitbol MM. Homozygous deletion in the coding sequence of the c-mer gene in RCS rats unravels general mechanisms of physiological cell adhesion and apoptosis. Neurobiol Dis. 2000; 7:586–599. [PubMed: 11114258]

Nandrot EF, Anand M, Almeida D, Atabai K, Sheppard D, Finnemann SC. Essential role for MFG-E8 as ligand for αvβ5 integrin in diurnal retinal phagocytosis. Proc Natl Acad Sci U S A. 2007; 104:12005–12010. [PubMed: 17620600]

Nandrot EF, Anand M, Sircar M, Finnemann SC. Novel role for αvβ5 integrin in retinal adhesion and its diurnal peak. Am J Physiol Cell Physiol. 2006; 290:C1256–C1262. [PubMed: 16338970]

Nandrot EF, Kim Y, Brodie SE, Huang X, Sheppard D, Finnemann SC. Loss of synchronized retinal phagocytosis and age-related blindness in mice lacking αvβ5 integrin. J Exp Med. 2004; 200:1539–1545. [PubMed: 15596525]

Singh S, D'Mello V, van Bergen en Henegouwen P, Birge RB. A NPxY-independent β5 integrin activation signal regulates phagocytosis of apoptotic cells. Biochem Biophys Res Commun. 2007; 364:540–548. [PubMed: 17963729]

Wayner E, Orlando R, Cheresh D. Integrins αvβ3 and αvβ5 contribute to cell attachment to vitronectin but differentially distribute on the cell surface. J Cell Biol. 1991; 113:919–929. [PubMed: 1709170]

Wu Y, Singh S, Georgescu MM, Birge RB. A role for Mer tyrosine kinase in αvβ5 integrin-mediated phagocytosis of apoptotic cells. J Cell Sci. 2005; 118:539–553. [PubMed: 15673687]

Young RW. The renewal of photoreceptor cell outer segments. J Cell Biol. 1967; 33:61–72. [PubMed: 6033942]

Young RW, Bok D. Participation of the retinal pigment epithelium in the rod outer segment renewal process. J Cell Biol. 1969; 42:392–403. [PubMed: 5792328]
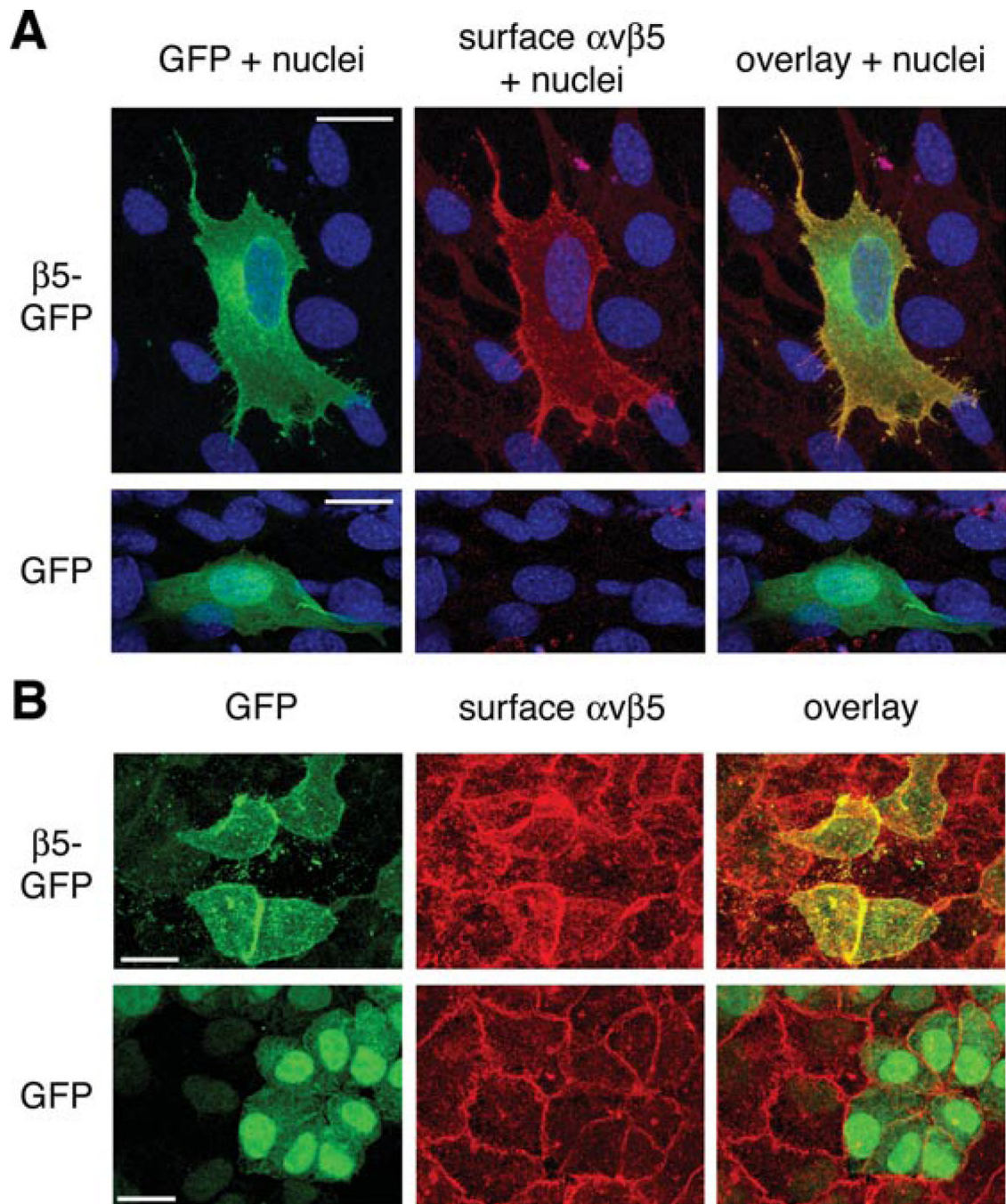
Figure 1. Human β5–GFP chimeric receptors with mouse or rat αv integrin traffic to the cell surface and distribute apically in RPE cells
Mouse 3T3 fibroblasts (**A**) or polarised rat RPE-J cells (**B**) transfected with either β5–GFP or control GFP-expressing plasmids as indicated were labelled live with αvβ5 receptor antibody. (**A**) αvβ5 antibody labelling (red) overlaps with GFP signals (green) at the cell surface 3T3 fibroblasts transfected with β5–GFP but not with GFP. Scale bars, 20 μm. (**B**) RPE-J cells expressing β5–GFP (green) show increase in surface αvβ5 antibody (red) compared with untransfected neighbouring cells or to GFP-expressing control cells. Scale bars, 8 μm.
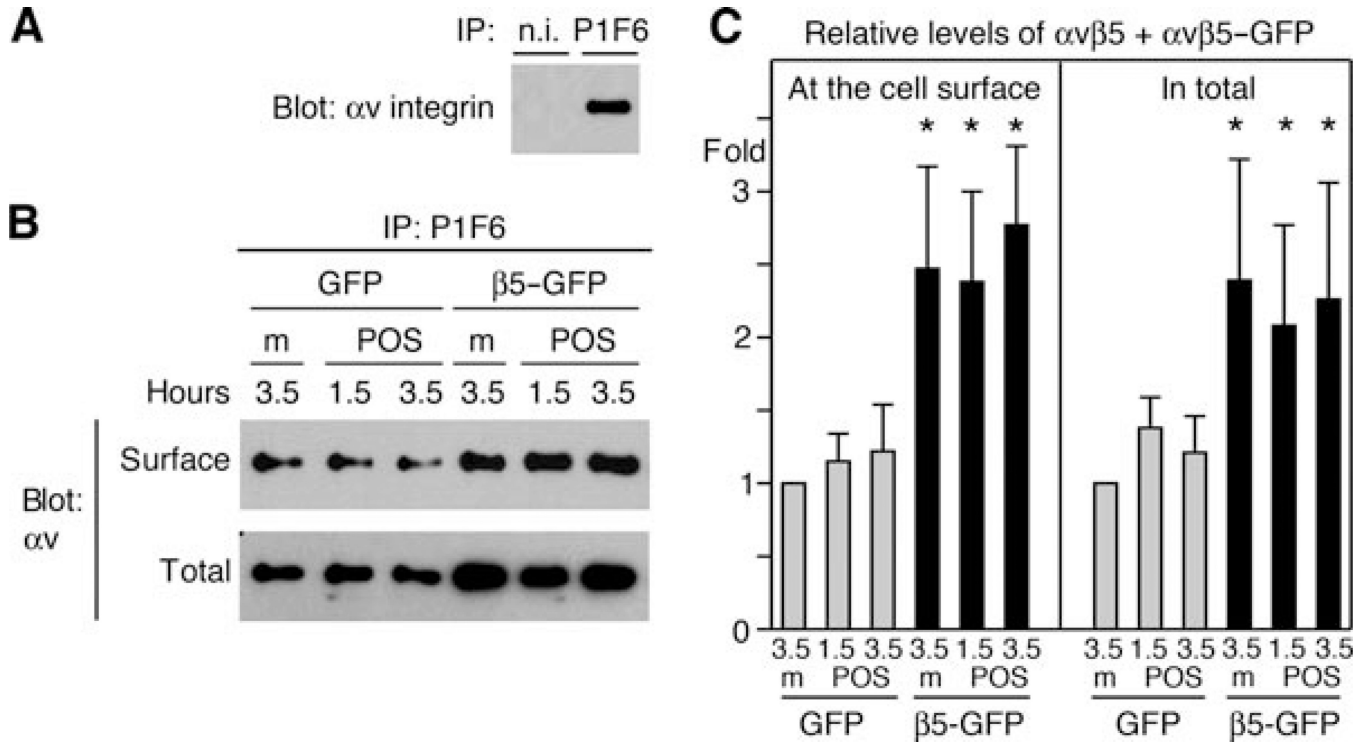
Figure 2. β5–GFP expressing adenovirus equally increases cell surface and total cellular levels of αvβ5/β5–GFP receptors

Surface and total αvβ5 integrin receptors in RPE-J cells after 1.5- and 3.5-h incubations with either medium or POS. (**A**) αv protein detected in immunoprecipitation assays is due to binding to the αvβ5 receptor antibody as non-immune (n.i.) IgG does not isolate αv. (**B**) Immunoprecipitations with αvβ5 receptor antibody isolate increased levels of αv protein from RPE-J cells infected with β5–GFP adenovirus as compared with GFP control virus, regardless whether surface proteins (panel surface) or total cellular proteins (panel total) are analysed. Panels show representatives of four experiments performed independently. Incubation with POS for 1.5 or 3.5 h as indicated does not affect levels of surface or total αvβ5 integrin receptors compared with incubation with medium (m). (**C**) Quantification of all immunoprecipitation experiments shows increases of 2.5 ± 0.7-fold and 2.4 ± 0.8-fold for surface αvβ5 and total αvβ5, respectively, in cells over-expressing β5–GFP as compared with GFP. Bars represent mean ± SEM. $n = 4$, $P < 0.05$.
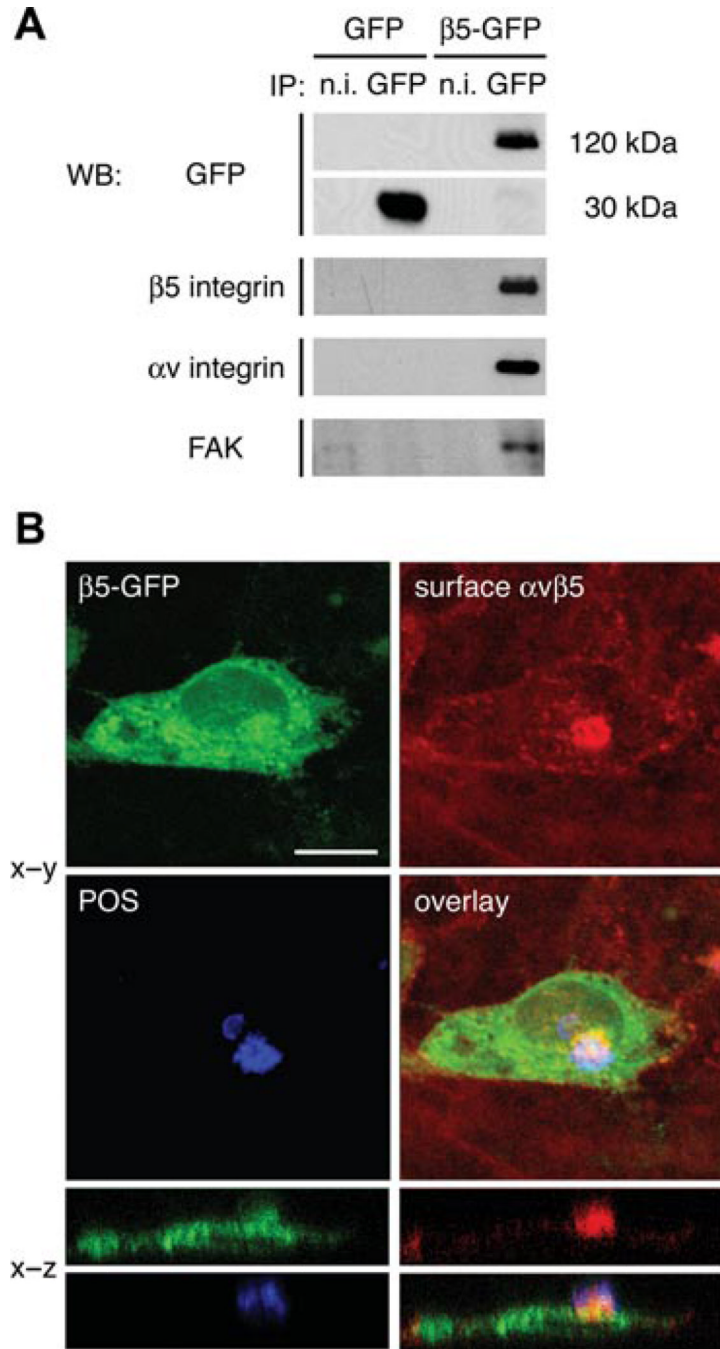
Figure 3. αvβ5–GFP receptors recruit FAK and co-localise with surface-bound POS
(**A**) Immunoblotting with antibody probes as indicated shows that immune complexes isolated with GFP antibodies contain αv, β5–GFP and FAK on cells over-expressing β5–GFP. Integrins or FAK do not co-precipitate with GFP antibody in cells expressing soluble GFP. Non-immune (n.i.) control antibody does not isolate any of the proteins tested. (**B**) Triple fluorescence labelling of a representative RPE-J cell expressing β5–GFP (green), labelled live in the cold with αvβ5 receptor antibody (red) followed by fixation and labelling with anti-POS antibody (blue) detects recruitment of αvβ5–GFP receptors to sites of surface-bound POS. x–y maximum projection and reconstructed x–z single scan

illustrates that β5–GFP protein (green) and apical αvβ5 receptors (red) localise beneath a surface-bound POS particle. Scale bar, 10 μm.
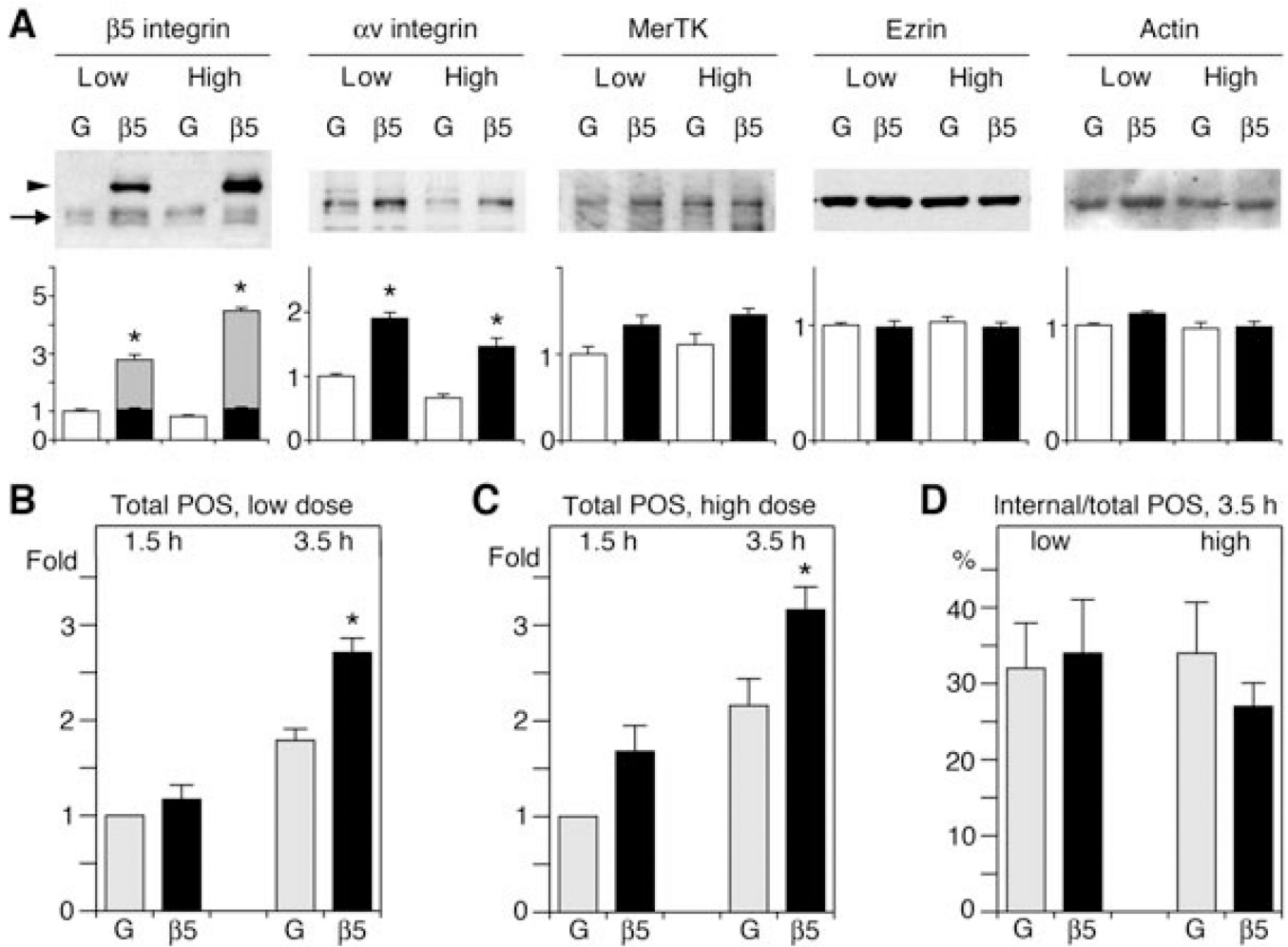
Figure 4. β5–GFP over-expression fails to proportionally increase POS binding and has no effect on internalisation by RPE-J cells

(**A**) Representative immunoblots showing individual samples of RPE-J cells over-expressing GFP (lanes G) or β5–GFP (lanes β5) at high or low levels as indicated. The same blot membrane is shown, probed sequentially with different antibodies as indicated. Increasing total β5 integrin content by β5–GFP over-expression significantly increases steady-state protein levels of αv integrin but not MerTK, ezrin or actin. In the β5 panel, arrowhead indicates band representing β5–GFP, arrow indicates band representing endogenous, untagged β5. Bar graphs below each blot show corresponding relative protein quantities with protein content of cells expressing low levels of GFP set as 1 (mean ± SEM, $n = 5$). Asterisks indicate significant difference in test protein quantity of β5–GFP expressing samples compared with appropriate low or high GFP expressing sample, with $P < 0.05$. In the β5 panel, black and grey bars represent endogenous β5 and over-expressed β5–GFP subunits, respectively. (**B and C**) RPE-J cells expressing either low (**B**) or high (**C**) levels of GFP (G, grey bars) or of β5–GFP (β5, black bars) were challenged with POS for 1.5 or 3.5 h before quantification of total (bound plus internal) POS by fluorescence scanning. Bars show total POS relative to total POS acquired by GFP expressing cells by 1.5 h, which is set as 1 (mean ± SEM, $n = 4$). Asterisks indicate significant difference of total POS in β5–GFP expressing cells as compared with GFP expressing cells at the same time point, $P < 0.05$. (**D**) β5–GFP expression did not significantly affect internalisation ratio, regardless of dose. Bars

show fractions of internalised POS of total POS in cells expressing low or high levels of GFP (G, grey bars) or of β5–GFP (β5, black bars) after 3.5 h of POS challenge as indicated (mean ± SEM, n = 3–4).
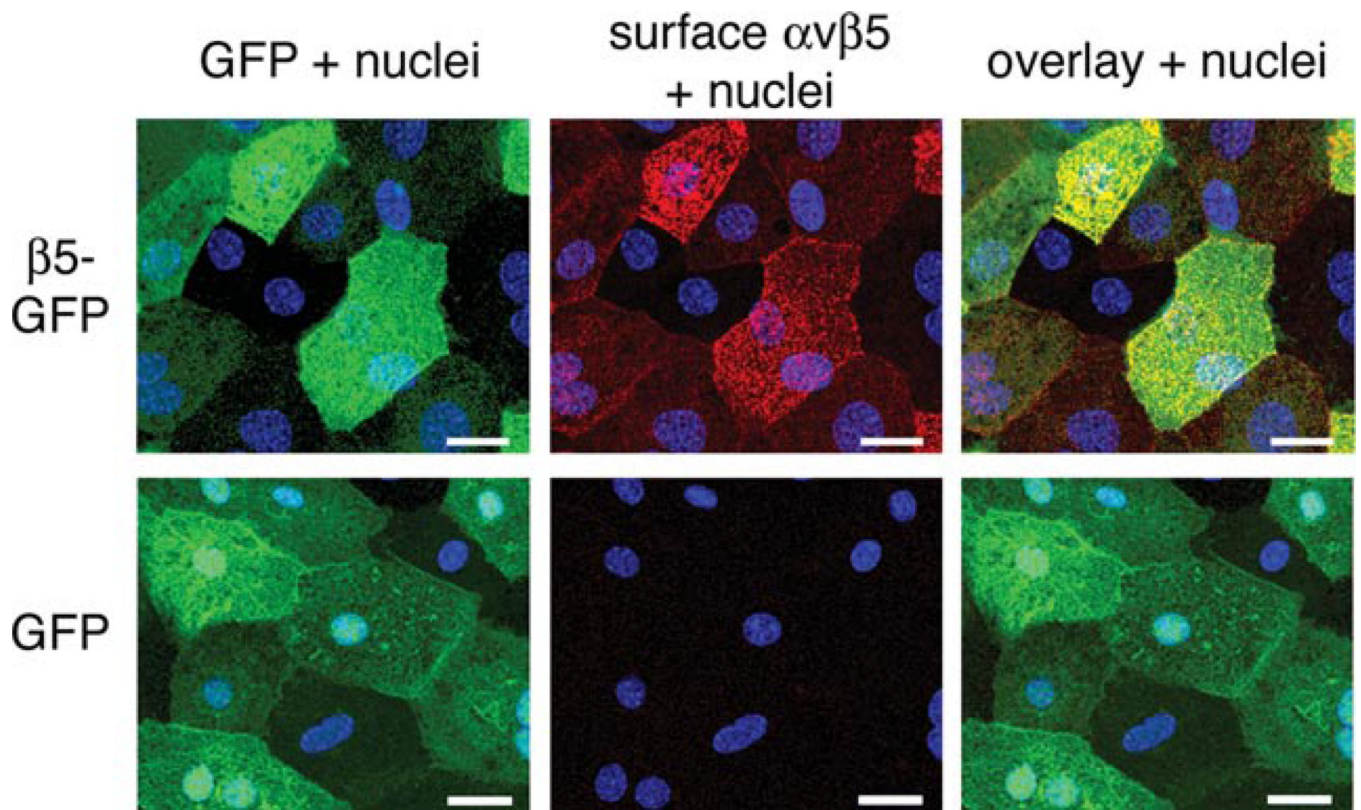
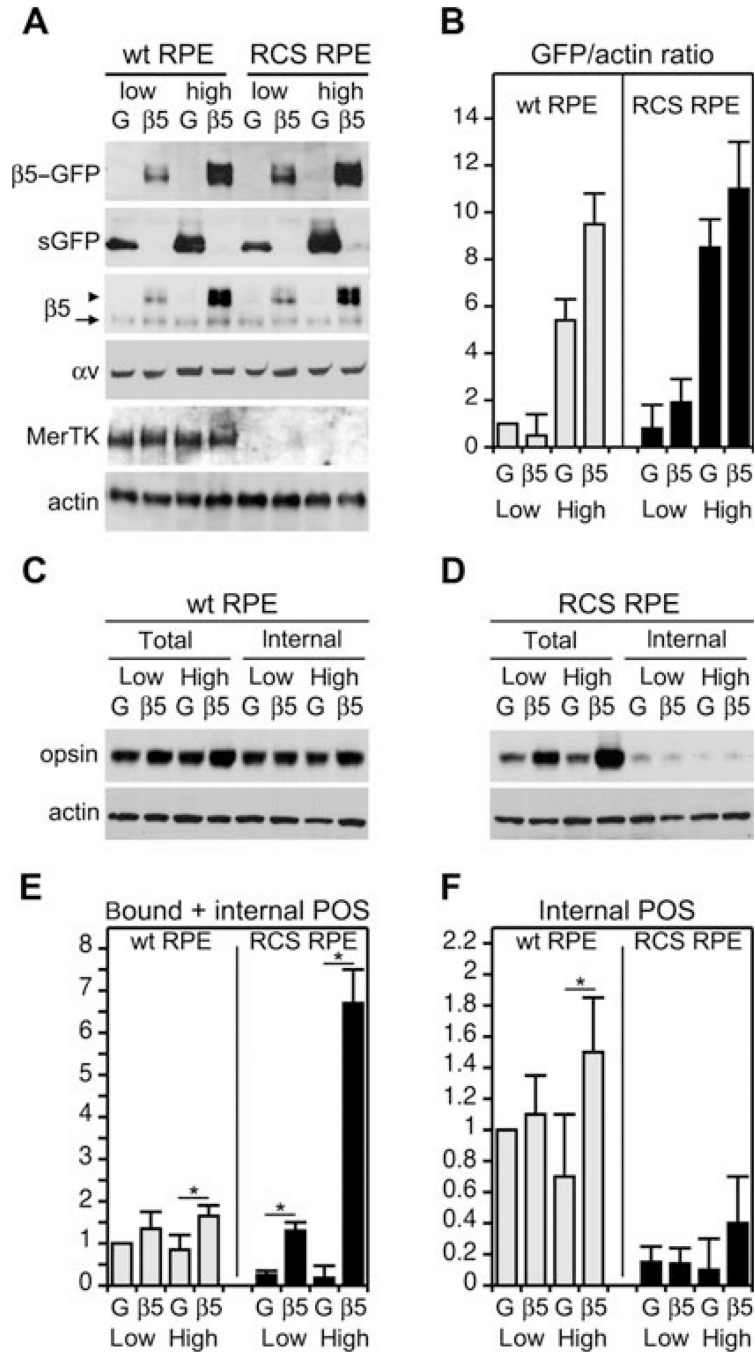**Figure 5. Expression of β5–GFP restores αvβ5 integrin receptor expression at the apical surface of β5−/− RPE in primary culture**
Primary, unpassaged β5−/− RPE cells were infected with high dose β5–GFP (top row) or GFP (bottom row) virus, live labelled with αvβ5 heterodimer-specific antibody and fixed. Representative maximal projections show GFP (green), indirect immunofluorescence of αvβ5 (red) and cell nuclei (blue). Scale bars, 20 μm.
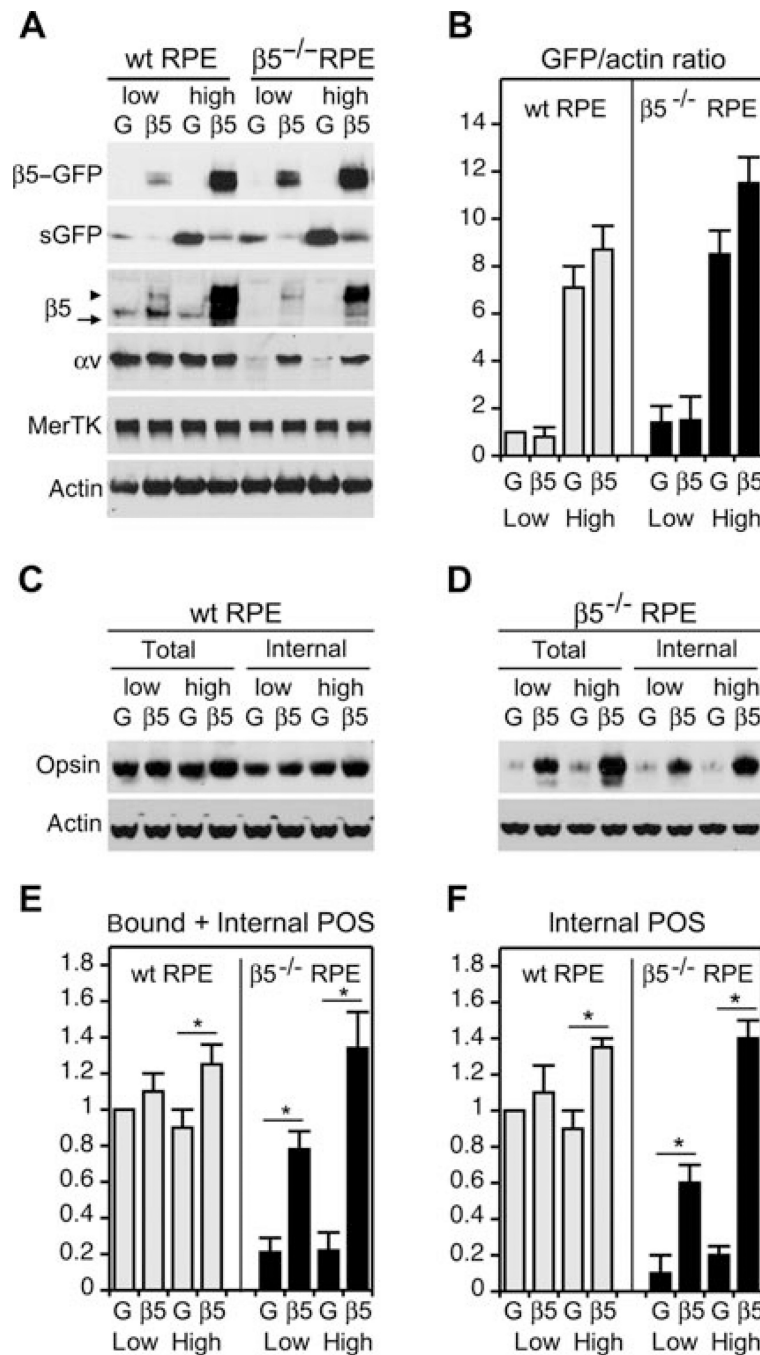
Figure 6. Expression of β5–GFP is sufficient to restore POS binding and internalisation by β5$^{-/-}$ mouse RPE but has little effect on wt mouse RPE

(**A**) Unpassaged primary RPE from wt or β5$^{-/-}$ mice were infected to express low or high levels of GFP (G) or of β5–GFP (β5), as indicated. Immunoblots of whole cell lysates show expression of low and high levels of exogenous proteins as expected, but no effect on expression of MerTK or actin. (**B**) Relative quantification of GFP bands compared with actin bands in each sample. Values are normalised to low GFP/actin, which is set as 1 (mean ± SD, $n = 3$). (**C**) Wt RPE expressing low or high levels of GFP or β5–GFP as indicated and as in (**A**) were fed isolated POS for 1.5 h. Total (bound plus internalised) POS were detected by opsin immunoblotting. Internal POS were detected by lysing cells following removal of

bound POS using EDTA. (**D**) Detection of total or internalised POS by β5$^{-/-}$ RPE by opsin blotting as in (**C**). (**E**) Quantification of total POS uptake by wt (grey bars) or β5$^{-/-}$ RPE (black bars). Bars represent mean relative POS opsin± SD compared with POS opsin detected in wt RPE expressing low GFP, which is set as 1. Asterisks indicate significant difference ($n = 3$, $P < 0.05$) comparing β5–GFP expressors with the appropriate GFP control. (**F**) Quantification of POS internalisation by wt (grey bars) or β5$^{-/-}$ RPE (black bars). Presentation and statistical analysis were performed as described in (**E**).

Figure 7. Expression of β5–GFP has little effect on POS uptake by wt rat RPE but causes excess POS binding by MerTK-deficient (RCS) rat RPE, which does not engulf bound POS
(**A**) Unpassaged primary RPE from wt or RCS rats were infected to express low or high levels of GFP (G) or of β5–GFP (β5) as indicated. Immunoblots of whole cell lysates show expression of low and high levels of exogenous proteins as expected, but no effect on expression of MerTK or actin. (**B**) Relative quantification of GFP bands compared with actin bands in each sample. Values are normalised to low GFP/actin, which is set as 1 (mean ± SD, *n* = 3). (**C**) Wt RPE expressing low or high levels of GFP or β5–GFP as in (**A**) received isolated POS for 1.5 h. Total (bound plus internalised) POS were detected by opsin immunoblotting. Internal POS were detected by lysing cells following removal of bound

POS using EDTA. (**D**) Detection of total or internalised POS by RCS RPE by opsin blotting as in (**C**). (**E**) Quantification of total POS uptake by wt (grey bars) or RCS RPE (black bars). Bars represent mean relative POS opsin ± SD compared with POS opsin detected in wt RPE expressing low GFP, which is set as 1. Asterisks indicate significant difference ($n = 3$, $P <$ 0.05) comparing β5–GFP expressors with the appropriate GFP control. (**F**) Quantification of POS internalisation by wt (grey bars) or RCS RPE (black bars). Presentation and statistical analysis were performed as described in (**E**).
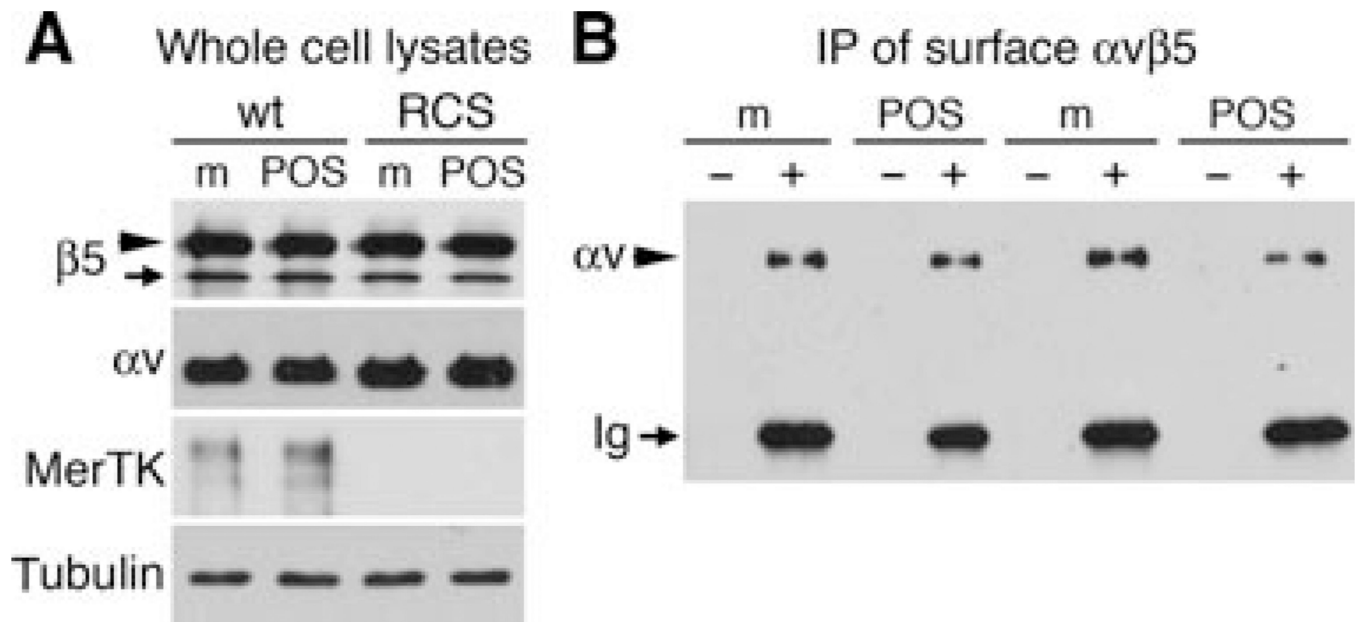
Figure 8. Levels of surface αvβ5 receptors formed by wt and RCS rat RPE upon over-expression of β5–GFP are similar and change little upon POS challenge
Wt or RCS rat primary RPE cells expressing high levels of β5– GFP were challenged with medium (lanes m) or POS (lanes POS) for 1.5 h. (**A**) Immunoblots of whole cell lysates show that wt and RCS rat RPE express equal levels of β5–GFP and β5 (panel β5, arrowhead indicates β5–GFP, arrow indicates endogenous β5) and αv integrin. MerTK blot confirmed genotype of animals. Tubulin blot served as loading control. (**B**) Live surface immunoprecipitations with αvβ5 receptor antibody isolate equal levels of αv protein from wt and RCS RPE fed with medium or POS. Panels are representatives of three experiments performed independently. Quantification of surface immunoprecipitation experiments did not reveal significant differences between surface receptor levels of wt and RCS RPE, regardless of phagocytic challenge ($n = 3$, $P > 0.1$).
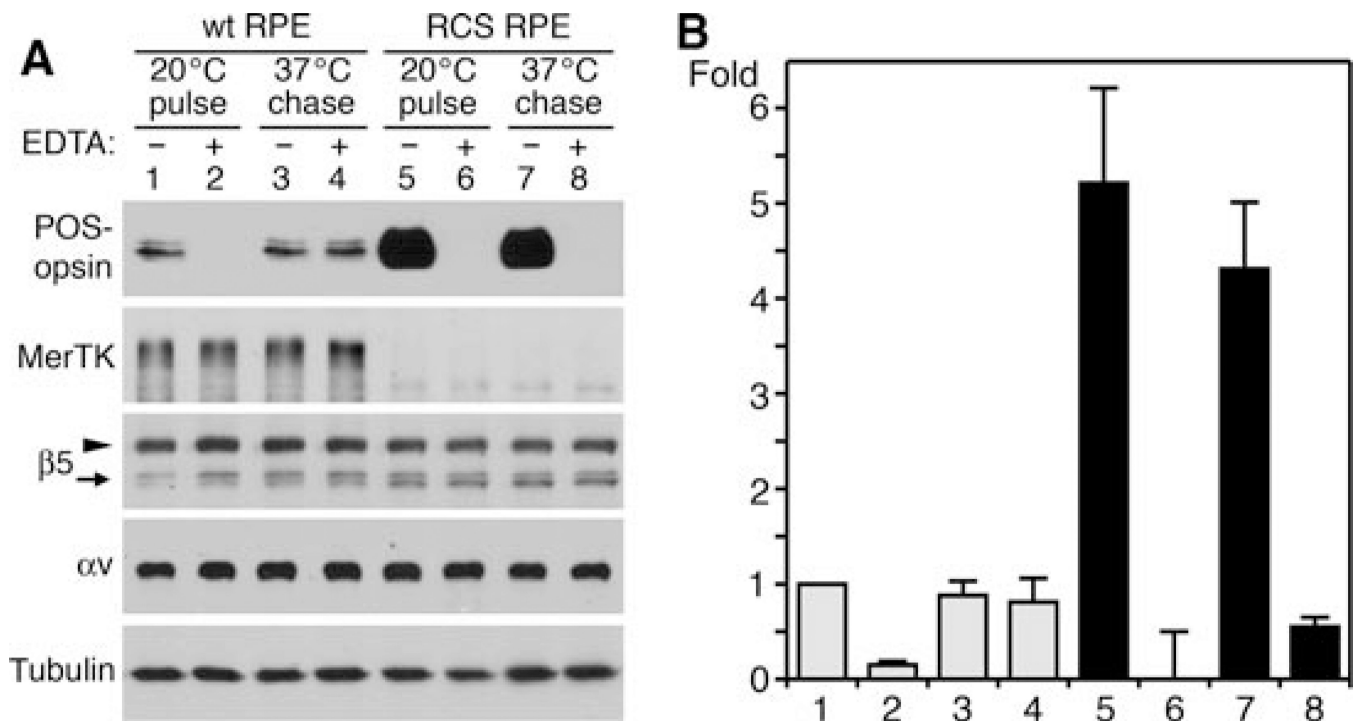
Figure 9. Expression of β5–GFP increases RCS binding of POS significantly more than that of wt RPE even if POS internalisation is inhibited by incubating at 20°C

Pulse–chase phagocytosis assays of wt and RCS RPE expressing high levels of β5–GFP as characterised in Figure 8. (**A**) Representative immunoblots detecting total and internalised POS-opsin, receptor proteins and tubulin in whole cell lysates of samples as indicated. Internal POS were detected by lysing cells following removal of bound POS using EDTA, lanes as indicated. Lanes 1, 2, 5 and 6 show cells fed with POS for 1 h at 20°C, which allows POS binding but not engulfment (pulse). Lanes 3, 4, 7 and 8 show cells pulsed with POS for 1 h at 20°C followed by removal of unbound POS and continued incubation for 1 h at 37°C, which allows engulfment (chase). (**B**) Quantification of total (odd bars) and internal (even bars) POS in samples numbered as in (**A**). Grey bars, wt RPE, black bars, RCS RPE. Bars show mean ± SD fold POS uptake relative to total POS of wt RPE after the pulse (bar 1), which was set as 1 ($n = 3$). Wt but not RCS RPE completely engulfs bound POS during the chase (compare 4 to 3). Equal levels of total POS bound during the pulse and internal POS after the chase indicate that there is no degradation of POS during the experiment (compare 3 to 1). RCS RPE binds significantly more POS than wt RPE during the pulse (compare 5 to 1, $P < 0.001$). As expected, POS of RCS RPE remain largely surface bound during the chase (compare 7 to 8).
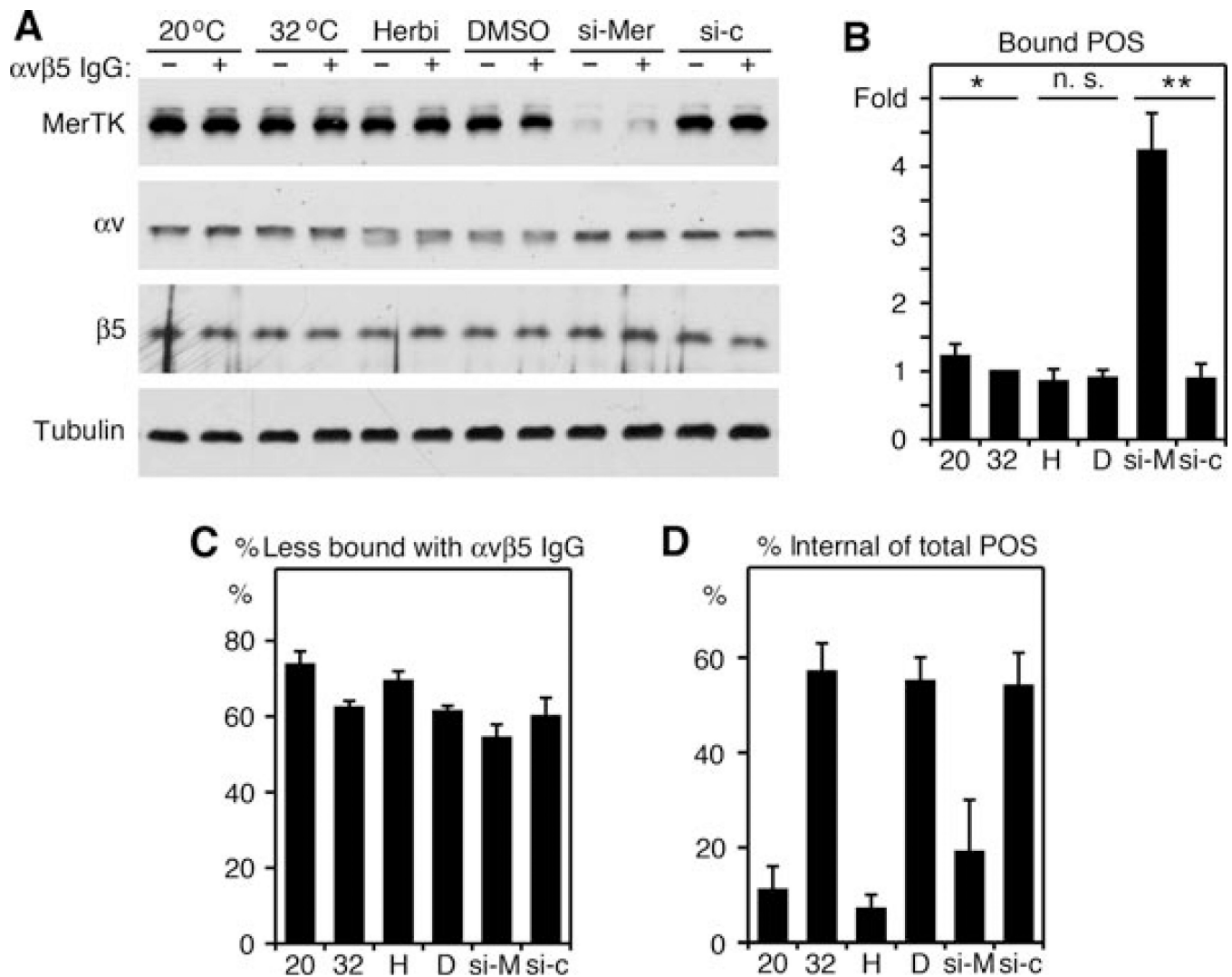
Figure 10. Decreasing MerTK protein levels but not non-specific inhibition of internalisation by 20°C incubation temperature or pharmacological inhibition of tyrosine kinases increases binding of POS by endogenous αvβ5 integrin receptors of RPE-J cells

RPE-J cells were incubated at 20°C or 32°C, or at 32°C in the presence of Herbimycin A (Herbi, H) or DMSO solvent (D), or at 32°C after receiving MerTK-specific (siMer, si-M) or control siRNA (si-c) for 2 days. Cells were harvested after POS challenge for 3.5 h in the presence of non-immune IgG (lanes –) or αvβ5 receptor antibody (lanes +). (**A**) Representative immunoblots showing whole cell lysates. (**B**) Graph shows quantification of bound POS determined by subtracting internal from total POS detected by fluorescence scanning. Bars show fold bound POS relative to bound POS acquired by untreated cells incubated at 32°C, which is set as 1 (mean ± SEM, $n = 3$). [*] indicates $P < 0.05$, [***] indicates $P < 0.005$ for differences of samples to specific appropriate controls as connected by black bars in the graph. (**C**) Graph showing percent inhibition of POS binding by αvβ5 antibody as compared with non-immune control antibody. αvβ5 antibody diminished POS binding by all samples including the increased binding by cells with downregulated MerTK, indicating that binding employed αvβ5 receptors. (**D**) Graph showing percent of internal POS of total POS. 20°C incubation, Herbimycin A and MerTK knockdown reduced the fraction of internal POS as compared with the specific appropriate control confirming that these treatments were effective as expected. [**] indicates significant difference with $P < 0.005$.